Postprint of: Galiński B., Wagner-Wysiecka E., Pyrrole bearing diazocrowns: Selective chromoionophores for lead(II) optical sensing, SENSORS AND ACTUATORS B-CHEMICAL Vol. 361 (2022), 131678, DOI: 10.1016/j.snb.2022.131678

Pyrrole bearing diazocrowns: selective chromoionophores for lead(II) optical sensing

Błażej Galiński, Ewa Wagner-Wysiecka*

Department of Chemistry and Technology of Functional Materials, Faculty of Chemistry, Gdańsk University of Technology, Narutowicza 11/12, 80-233 Gdańsk, Poland

* Corresponding Author

Tel.: +48 347 23 59

e-mail: ewa.wagner-wysiecka@pg.edu.pl

Abstract

Diazocrowns of 18-, 21- and 23-membered rings with pyrrole residue as a part of macrocycle were for the first time used as chromoionophores in lead(II) selective optodes. Sensing properties of optodes depend on the type of macrocycle, namely its size and the type of linker: oligoether or hydrocarbon chain.

The best results were obtained for optode bearing 18-membered crown with oligoether linker showing linear response range of 8.05×10^{-8} - 2.24×10^{-5} M lead(II) and detection limit of 1.15×10^{-8} M. Membrane, based on cellulose triacetate, is lead(II) selective giving color change from red to different shades of blue (pH 5.5). Results obtained for model and real samples of lead(II) showed that easily accessible and regenerable sensor material can be used for spectrophotometric and colorimetric (Digital Color Analysis) detection and determination of lead(II).

Keywords: chromoionophore; macrocycle; optode; cellulose triacetate; lead(II)

1. Introduction

Common environmental pollutant is lead and its salts. Lead(II) has a negative influence on human's health, but also on animals and plants, which are an integral part of our environment [1-11]. Although lead and its salts were almost eliminated from many areas of life and technologies, the Notre-Dame de Paris fire broke out on 15 April 2019 had risen fears about the potential lead(II) intoxication as a result of melting of 410 tons of lead from roof construction and spire of the cathedral. Harmful lead and its compounds can enter the body directly by respiration or by oral route with water or food. It was a reason for the preventive determination of the level of lead in blood in firefighters as well as its content in natural products such as honey [12-18]. Among others such situations need fast, reliable and importantly - field methods of lead detection and determination of the level of contamination.

Various types of sensors are used nowadays in many fields including control of industrial processes, environmental monitoring, clinical analysis and objects of everyday use, including food quality control [19-22]. Widely used are optical sensors due to their relative simplicity coming along with ensuring the accuracy, precision of indications [23-29] and the possibilities of analysis by digital color sensing - Digital Color Analysis (DCA) [30-33]. Selective optical sensors can be obtained among others by use of a selective (chromo)ionophore [34,35] immobilized in the receptor layer. It allows detection and determination of various chemical species in different types of samples and concentration levels (however, the determination of analytes in highly colored samples can sometimes be difficult). Optical sensors are important analytical tool, e.g. in medical diagnostics, clinical and environmental analysis [36-46]. Good candidates for ionophore-based optical sensors seem macrocyclic azocompounds due to relatively simple synthesis, spectral properties and discrimination of analyte according its size [47].

Our studies [48-50] showed that azomacrocyclic derivatives bearing pyrrole residue are lead(II) selective in acetonitrile and mixture of this solvent with water, but also are good lead(II) ionophores when used as ion-carriers in ion selective electrodes. Since that time other derivatives of this class of compounds were obtained and investigated as chromo(fluoro)ionophores [51,52]. Recently, we have investigated the effect of the exchange of oligoether fragment (18- and 21-membered crowns **1** and **2**, Fig.1) by hydrocarbon chain in 18- and 23-membered crowns **3** and **4** (Fig.1) on metal cation complexation [53].

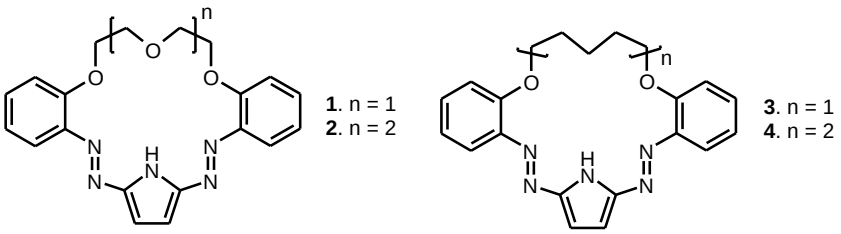

Fig. 1. Diazocrowns **1** - **4** [48,50,53] with pyrrole moiety in macroring.

Compounds **1**-**4** form stable complexes with lead(II) of 3:2 stoichiometry (crown:Pb) in acetonitrile which has been lastly confirmed by mass spectrometry [53]. Lead(II) complexation in acetonitrile and its mixture with water is related to a large spectral shift in UV-Vis absorption spectra observed as a distinct color change of solution from red-orange to blue. Crown **3** was proposed as a selective lead(II) probe in acetonitrile:water mixture with detection limit 56 μg/L. Preliminary studies showed that macrocycles can serve as chromoionophores in optical sensor layers for lead(II) detection in aqueous solution.

In this research, for the first time, four diazobenzocrowns **1**-**4** with pyrrole residue as an integral part of macrocycle were immobilized in a cellulose triacetate (CTA) membrane and were investigated as chromoionophores for lead(II) selective optodes. The spectrophotometric response of prepared optodes towards lead(II) aqueous solution was investigated regarding the influence of membrane composition and pH of solution on the response time, life-time and reversibility of sensor layer, detection limit and linearity of response. Digital Color Analysis (DCA) approach as competing to spectrophotometric measurements was also proposed.

2. Materials and methods

2.1. Chemicals

Chromoionophores **1**-**4** (Fig. 1) were prepared according to the previously reported methods [48,53]. Identity of compounds was confirmed by comparison of spectral and TLC data with data for genuine samples of macrocycles deposited in our lab.

Cellulose triacetate (CTA) was acquired from Acros Organics. Triethylene glycol ≥99.0% (TEG) was obtained from Merck (Germany). Bis(1-butylpentyl) adipate ≥98.0% (BBPA), dibutyl phthalate ≥99.0% (DBP), bis(2-ethylhexyl) phthalate ≥99.5% (DOP), bis(2-ethylhexyl) sebacate ≥97.0% (DOS) and 2-nitrophenyl octyl ether ≥99.0% (NPOE) were purchased from Sigma Aldrich (Selectophore). Potassium tetrakis(4-chlorophenyl)borate ≥98.0% (KTClPB) was procured from Fluka (Selectophore). Dichloromethane, chloroform, 2-propanol, acetic acid, hydrochloric acid, disodium ethylenediaminetetraacetate dihydrate (EDTA-Na_2) and ethylenediamine (EDA) were purchased from POCh (Poland).

All aqueous solutions were prepared using ultra-pure water obtained by the reverse osmosis (RO) from Hydrolab Poland station (conductivity <1 $\mu S/cm^{-1}$). Nitric acid and sodium hydroxide (p.a.) used for adjusting pH of solutions were purchased from POCh (Poland). Aqueous stock solutions of salts (10^{-2} M) of $NaNO_3$ (≥99.8%), KNO_3 (≥99.8%), $Mg(NO_3)_2 \times 6H_2O$ (≥99.0%), $Ca(NO_3)_2 \times 4H_2O$ (≥99.0%), $Ni(NO_3)_2 \times 6H_2O$ (≥98.0%), $Zn(NO_3)_2 \times 6H_2O$ (≥98.0%), $Cd(NO_3)_2 \times 4H_2O$ (≥98.0%) from POCh (Poland) and $Cu(NO_3)_2 \times 3H_2O$ (≥99.5%) from Merck (Germany) as interfering ions were used. Stock solution (10^{-2} M) of Pb(II) was prepared by dissolving $Pb(NO_3)_2$ (≥99.0%, Alfa Aesar, Massachusetts, USA) (0.0331 g) in nitric acid (1 mL of 10^{-2} M) and diluting it in volumetric flask (10 mL) with deionized water. Working solutions containing Pb(II) were prepared by a serial dilution of the stock solution. For recovery studies Standard Reference Solution of lead(II) 1000 ppm (Merck) was used.

2.2. Instrumentation

All absorbance measurements were carried out using a Unicam UV-300 spectrometer in 1 cm quartz cuvettes (Starna® Brand). pH was monitored using pH-meter CPC-511 with glass electrode EPS-1 (ELMETRON, Poland). The concentration of metal ions in reference sample of real treated industrial wastewater was determined by ICP-OES iCAP 7400 Analyzer.

2.3. Membrane preparation

To obtain the best sensing membrane films in terms of maximum sensitivity towards Pb(II), it was necessary to optimize various experimental conditions. For this purpose four series (A-D, of optodes were prepared, all based on cellulose triacetate (250.0 mg), containing the respective plasticizer and chromoionophores **1, 2, 3** or **4**. Unfortunately membranes with compound **3** can't be obtained, because of crystallization of chromoionophore in the polymer matrix (Fig. S1).

Series A of membranes were based on different types of plasticizers (337.2 mg, d = 1.124 g/mL) and chromoionophore **1**, **2** or **4** (1.0 mg).

Series B of optodes were prepared using triethylene glycol - TEG (337.2 mg) as a plasticizer and different amounts of the respective chromoionophores (0.5 – 2.0 mg).

Series C of optodes contained varying amounts of TEG (168.6 – 505.8 mg), the respective amount of chromoionophores from series C and lipophilic salt KTClPB in amount corresponding to half mass of chromoionophores.

Series D of membranes consisted of TEG (337.2 mg), 1.0 mg of compounds **1** or **2** or 1.5 mg of compound **4** and different amounts of lipophilic salt KTClPB (0.25 – 1.00 mg).

The composition of membranes of series A-D with corresponding amounts of all membranes components are shown in Table S1.

All components of each optode from each series were dissolved in dichloromethane (6 mL) with continuous stirring using a magnetic stirrer for 2 h and ultrasonicated for 5 min – to form a clear solution. In the next step, solutions were poured on, prepared in advance (washed with nitric acid, deionized water, acetone and 2-propanol) petri dish (9 cm diameter), covered loosely with a lid and left for solvent evaporation. After 24 h obtained optode films were peeled off from the petri dish and cut into 0.9×4.5 cm strips. Blank membranes were prepared in an analogous way using all components besides chromoionophores and lipophilic salt.

2.4. Measurement procedures

2.4.1. Absorbance measurements

Before measurements, membranes were washed three times with deionized water to remove water-soluble additives from the surface. Then the membranes were placed in a quartz cuvette containing nitric acid solution (2.3 mL, 10^{-5} M) in the sample path of the spectrophotometer. Measurements were carried out against blank membranes in the reference path of the spectrophotometer. Then the content of the measurement cell was titrated with a solution of lead(II) nitrate.

In order to avoid the absorbance measurements errors resulting from possible heterogeneity of the optodes prepared in different series, the absorbance value measured at two wavelengths corresponding to the maximum absorbance of the chromoionophore and its complex with lead(II) is given as the spectral response. Then the response is expressed as the difference in absorbance ΔA for two wavelength and calculated using the formula: $\Delta A = (A_{\lambda maxPb}/A_{\lambda max}) - (A_{0\lambda maxPb}/A_{0\lambda max})$, where A_0 is absorbance before and A after contact with lead(II) salt, λ_{max} corresponds to maximum absorbance measured for membrane with chromoionophore and λ_{maxPb} is absorbance value at wavelength corresponding to maximum absorbance measured for membrane upon contact with lead(II) salt. Precisely: $A_{\lambda max}$ - the value of absorbance at 518 nm for membranes with azocrown **1** and at 508 nm for optodes with compounds **2** and **4**; $A_{\lambda maxPb}$ - the value of absorbance at 615 nm for membranes with azocrown **1** and at 587 nm for optodes with crowns **2** and **4**.

In competition studies the value of the signal generated by optode in the presence of lead(II) nitrate was recorded before (ΔA_0) and after (ΔA) addition of 10-fold molar excess of interfering metal salt. The influence of interfering ions on spectrophotometric response

towards lead(II) was expressed as the absolute value of relative response $RR\% = |[(\Delta A - \Delta A_0)/\Delta A_0]| \times 100\%$.

Limits of detection (LOD) were calculated using expression $LOD = 3\sigma/k$, where σ is the standard deviation of the blank and k is the slope of the linear function $\Delta A = f([Pb(II)])$.

All experiments were carried out in the presence of lead(II) nitrate concentration 10^{-4} M at nitric acid solution (pH 5.50±0.05).

2.4.2.Digital image colorimetry system

Digital images were captured in a photograph lightbox of white sides (16×10×20 cm) illuminated with 20 LEDs with a color temperature of 6000K (1.5 W) (Fig. S2). The focusing distance was fixed at 10 cm. Smartphone LG K10 with the Color Analysis application (CA) designed by Roy Leizer [54], was used for capturing digital images. Image data has been processed by cropping to a 260×780 pixels rectangular area of the image after immersing the optode in lead(II) nitrate solution. Obtained images were analyzed with a CA application giving the percentage of individual values of red (R), green (G) and blue (B) components of the pixels in the image. These values were saved in an Excel file and sent to a computer to calculate the intensity values of each color. Color change of optode given as ΔE_{RGB} [55-57] was calculated using equation: $\Delta E_{RGB} = [(R_0 - R)^2 + (G_0 - G)^2 + (B_0 - B)^2]^{1/2}$ where R_0, G_0 and B_0 values correspond to membranes dipped in deionized water of pH 5.5 (HNO_3), and R, G and B values correspond to color of membrane after immersing in lead(II) nitrate solution.

3. Results and discussion

3.1. Effect of the individual components of membrane on response value ΔA of the optodes towards lead(II)

Series A of optodes has been investigated in terms of the value of the generated signal depending on the type of plasticizer (Fig. 2a). Optodes were obtained using six most commonly used plasticizers: TEG, BBPA, DOS, NPOE, DOP and DBP. For these screening studies the same amount of each plasticizer i.e. 337.2 mg was used. The highest value of ΔA was obtained for all membranes using TEG. Therefore, this plasticizer was chosen for further studies.

To optimize the amount of chromoionophore, membranes with different quantities (0.5–2.0 mg) of diazocrowns **1**, **2** or **4** were prepared in a series B of membranes. The highest value of ΔA was obtained for optodes with 1.0 mg of compound **1** or **2** and 1.5 mg in the case of chromoionophore **4** (Fig. 2b). More than 1.0 mg of chromoionophore for membranes with

crowns **1** or **2** and 1.5 mg for sensor layer with compound **4**, causes the decrease of the observed signal. Worth noting is the highest, among investigated membranes, observed ΔA value for membrane with diazocrown **1** in all cases. Above mentioned quantities of chromoionophores were selected for further research.

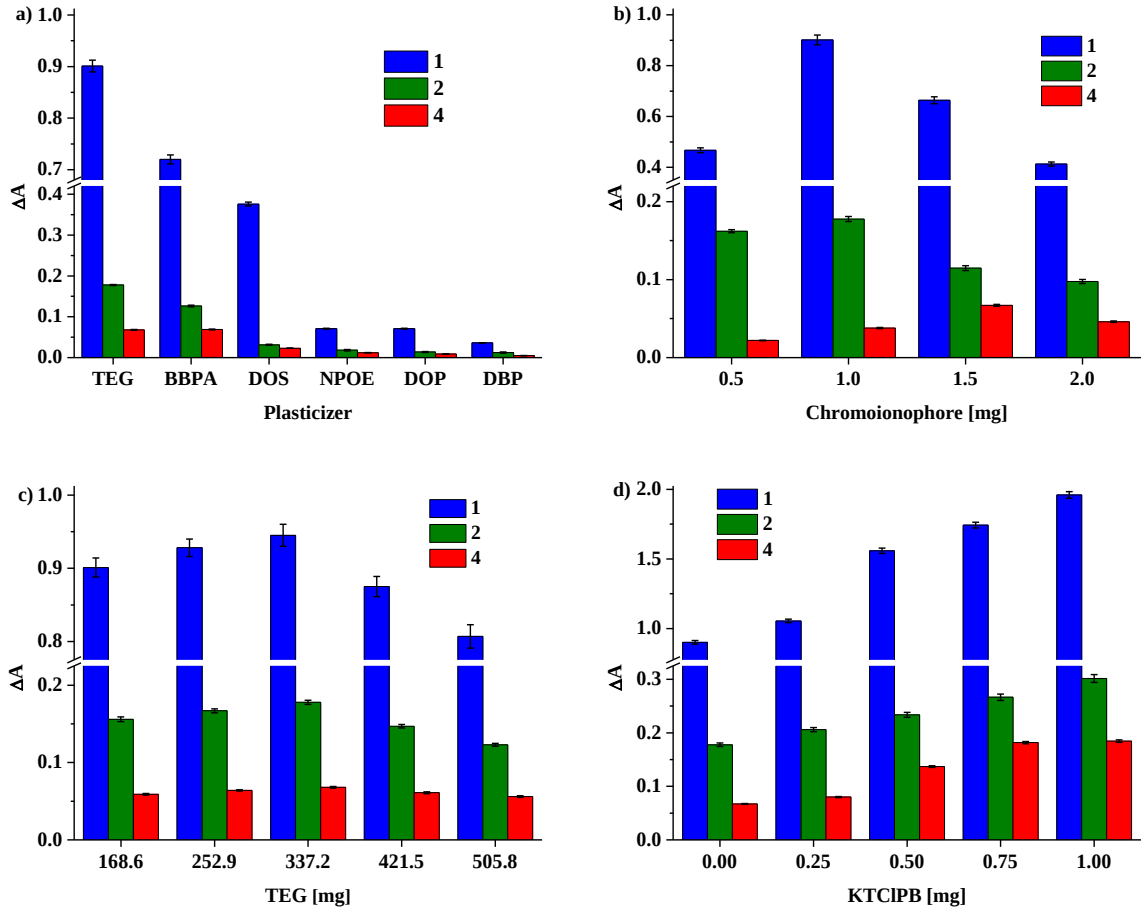

Fig. 2. The effect of a) type of plasticizer, b) amount of chromoionophore [mg], c) amount of TEG [mg] and d) amount of KTClPB [mg] on ΔA value (change of the optical signal, absorbance, in the presence of lead(II) salt) of optodes with chromoionophores **1**, **2** and **4**.

The amount of TEG does not significantly affect the optode response (Fig. 2c), however, triethylene glycol obviously affects the mechanical properties and membrane durability. For membranes with chromoionophore **1**, maximum amount of TEG is 168.6 mg (150 μl), otherwise the crown eluviation from polymer matrix occurs. For membranes with compounds **2** and **4**, the optimal amount of TEG seems to be 337.2 mg (300 μl). Above this quantity, a slight decrease of response and deterioration of the mechanical properties are noticeable and the membrane ceases to be stiff. The effect of lipophilic salt presence - KTClPB - and its amount (0.25–1.0 mg) on the value of the generated signal ΔA, was checked for the membranes from series B were compared with the optodes from series D. Fig. 2d shows that the highest increase of ΔA signal was obtained for membranes containing 1.0 mg of the

KTClPB. For optodes with compound **1** or **2**, the amount of lipophilic salt above 0.5 mg in the membrane, slightly increases the value of the detection limit, however enhances sensitivity (cf. Table S2). The same effect was noticed, when more than 0.75 mg of KTClPB was used in optodes with compound **4**. Having in mind the proposed model of the lead(II) binding by macrocycles **1**-**4** in acetonitrile [53] (realizing that complexation equilibrium can be a different process in pure organic solvent than in membrane) we assume possible functioning mechanism:

$$2Pb^{2+}_{(aq)} + 3LH_{(org)} + 2R^{-}_{(org)} \rightleftarrows (Pb_2L_3H)^{2+}_{(org)} + 2R^{-}_{(org)} + 2H^{+}_{(aq)}$$

where LH is chromoionophore, R^- is the anion of the lipophilic salt and $(Pb_2L_3H)^{2+}$ is a complex. It suggests chromoionophore/lipophilic salt ratio 1.5. On the other hand it was proved that complexes of various stoichiometry can be formed depending on the measurement conditions, e.g. mass spectra registration [53]. Taking all above into account, 0.5 mg of lipophilic salt was selected for further testing of membranes with crowns **1** or **2**, and 0.75 mg for polymer layers with crown **4** as a compromise between detection limit and the sensitivity of the sensing material.

The possible effect of solvent which is used for optode cocktail preparation was also investigated by dissolving all components of membranes in dichloromethane or in chloroform. Interestingly, it was found that membranes for which dichloromethane was used as solvent characterize larger ΔA values than these for which chloroform was used. All membranes obtained in chloroform showed a lower value of the generated signal (ΔA) than in dichloromethane, regardless of the composition of the receptor layer: type of plasticizer, amount of chromoionophore or amount of additive (Fig. S3a-c). It follows that the use of dichloromethane as a solvent for the preparation of optodes is a better choice (Fig. S4). This can be influenced by the solvent evaporation rate, and perhaps also a tendency to formation of complexes with dichloromethane by azomacrocyles confirmed by the X-ray structure in literature [48].

On the basis of above, for further studies we have chosen as an optimized composition of membranes the composition listed in Table 1.

Table 1. The optimized composition of membranes of optodes with diazobenzocrowns **1**, **2** and **4** as chromoionophores.

Optode	Chromoionophore		KTClPB		TEG		CTA	
	mg	wt%	mg	wt%	mg	wt%	mg	wt%
1	1.00	0.24	0.50	0.12	168.60	40.13	250.00	59.51
2	1.00	0.17	0.50	0.08	337.20	57.28	250.00	42.47
4	1.50	0.25	0.75	0.13	337.20	57.21	250.00	42.41

3.2. UV-Vis spectral characterization of optodes

The response of optodes of composition shown in Table 1 towards lead(II) was investigated spectrophotometrically (Fig. 3). UV-Vis spectra of optodes with crowns **1**, **2** and **4** before contact with lead(II) are similar to spectra of these macrocycles registered in highly apolar solvent - acetonitrile [48,50,53]. Electronic spectra exhibit bands which can be attributed to $\pi \rightarrow \pi^*$ (~390 nm) and $\pi \rightarrow \pi^*$and/or $n \rightarrow \pi^*$ (~500 nm) electronic transitions typical for chromophore systems with azo group(s) connecting aromatic rings [58]. The spectrophotometric response of optodes in the presence of lead(II) nitrate characterizes with the appearance of a new, bathochromically shifted absorbtion band, which intensity increases with the increasing concentration of lead(II) nitrate (Fig. 3). The maximum of absorption of the optodes with diazocrown **1** is located at 518 nm and for **2** and **4** it is at 508 nm, and is shifted towards 615 (for **1**) and 587 nm (for **2** and **4**) when titrated with aqueous solution of lead(II) nitrate. It is consistent and comparable with spectral and color changes resulting from the formation of complex of 3:2 stoichiometry when titrating acetonitrile solutions of crowns **1**, **2** and **4** with lead(II) perchlorate [50,53]. Thus it can be assumed that the observed spectral pattern for optodes can be a result of the complex formation between macrocyclic chromoionophore entrapped in a polymeric matrix and lead(II) nitrate.

Comparing the obtained results shown in Fig. 3 it is quite well seen that spectral changes - the highest increase of optical signal and the highest spectral shift - are the most pronounced for optodes with crown **1**.

The properties of ion-selective membranes are the result of many factors. The sensing mechanism depends mainly on the properties of ionophore such as its lipophilicity, shape, molar mass and the value of stability constant of complex with target ion. Other membrane components, namely membrane solvent - plasticizer, polymer matrix or ionic additives also affect the characteristics of the sensor layer.

Used by us chromoionophores are macrocyclic compounds of similar structure: two azo groups and pyrrole moiety as parts of macrocycle. The difference is that two of them bear an oligoether chain (**1** and **2**) and in the case of two other (**3** and **4**) ring closure is achieved by introducing hydrocarbon linkage (Fig.1). Differences in the length of above linkages result in various macrocycle size, namely 18-memebred - compounds **1** and **3**, 21- for **2** and 23-membered in case of **4**. The change of linker type obviously affects the lipophilicity of macrocycles (Table S3, Fig. S5). The highest value ($logP_{TLC}$) 9.42±0.03 was determined for

23-membered crown **4** (ten carbon atoms linkage) and the lowest 5.54±0.05 for 18-membered crown **1** (oligoether moiety).

Macrocycles, as it was reported by us earlier [48,50,53] form in aprotic dipolar solvent - acetonitrile complexes with lead(II) of 3:2 stoichiometry (crown:lead(II)) of relatively high values of stability constants (Table S3, Fig. S5). The highest value of logK 21.10±0.09 was found for complex formed by 21-membered crown **4**, the lowest 18.10±0.01 for 18-membered macrocyle **1**.

Chromogenic crowns **1**, **2** and **4** were successfully incorporated into cellulose triacetate membrane - a polymer matrix of a moderate hydrophobicity [59,60] plasticized with a polar, hydrophilic triethylene glycol. The relative compatibility in hydrophobic/hydrophilic nature between membrane matrix and crown **1** of relatively high, however the lowest, lipophilicity among studied here macrocycles may be one of the reasons for the most promising properties of the obtained sensing layer.

The sensor properties are also dependent on the cation exchange equilibrium between organic (membrane) and aqueous phase, which is on the other hand dependent on the complex formation constant in polymeric matrix [61]. The formation of very stable complexes of relatively high formation constants connected with low dissociation rate usually precludes the use of the particular compound as an effective ionophore in membrane systems. Although given above stability constant values of lead(II) complexes of crowns used here as chromoionophores were determined in acetonitrile, and having in mind that the complex formation unnecessarily must be analogous in polymer membrane, it may be seen that strength of the host-guest interaction correlates with the obtained results for fabricated by us optodes. Namely, more promising in regard to the generated optical signal is optode in which crown **1** of the lowest value of stability constant was used. One more factor connected with the properties of the ionophore and its complex with target ion influencing on optode characteristics, which may be taken under consideration is molar mass. Lower molar mass enables higher mobility in the membrane – which also speaks in favor of using compound **1** as chromoionophore in proposed lead(II) selective optodes.

The effect of the presence of ion-exchange sites as additive components of membranes on the properties of both ion-selective electrodes and optodes was widely discussed in literature as their presence influence the characteristics of sensors [e.g. 62-65] . The positive effect of the use of the lipophilic additives is usually connected among the others with the sensitivity improvement, increasing of the selectivity for divalent over monovalent ions, reduction of the response time, but it was also shown that higher amounts of these components may result in

deteriorated detection limit due to increased ion flux across the membranes [66,67]. These and some other reasons discussed in details by Simon and co-workers [62] point, that the components of carrier-based ion-selective electrodes must be chosen very carefully.

The properties of the optodes with crowns **1**, **2** and **4** as chromoionophores are probably the synergistic effect of all mentioned above factors and likely some others, not predicted, connected with the specificity of the investigated system. Thus at this stage, it seems hardly to postulate which of them is dominating. The choice of the membrane of the proposed composition was the compromise among the values of the generated optical signal, linear response range, reversibility and detection limit.

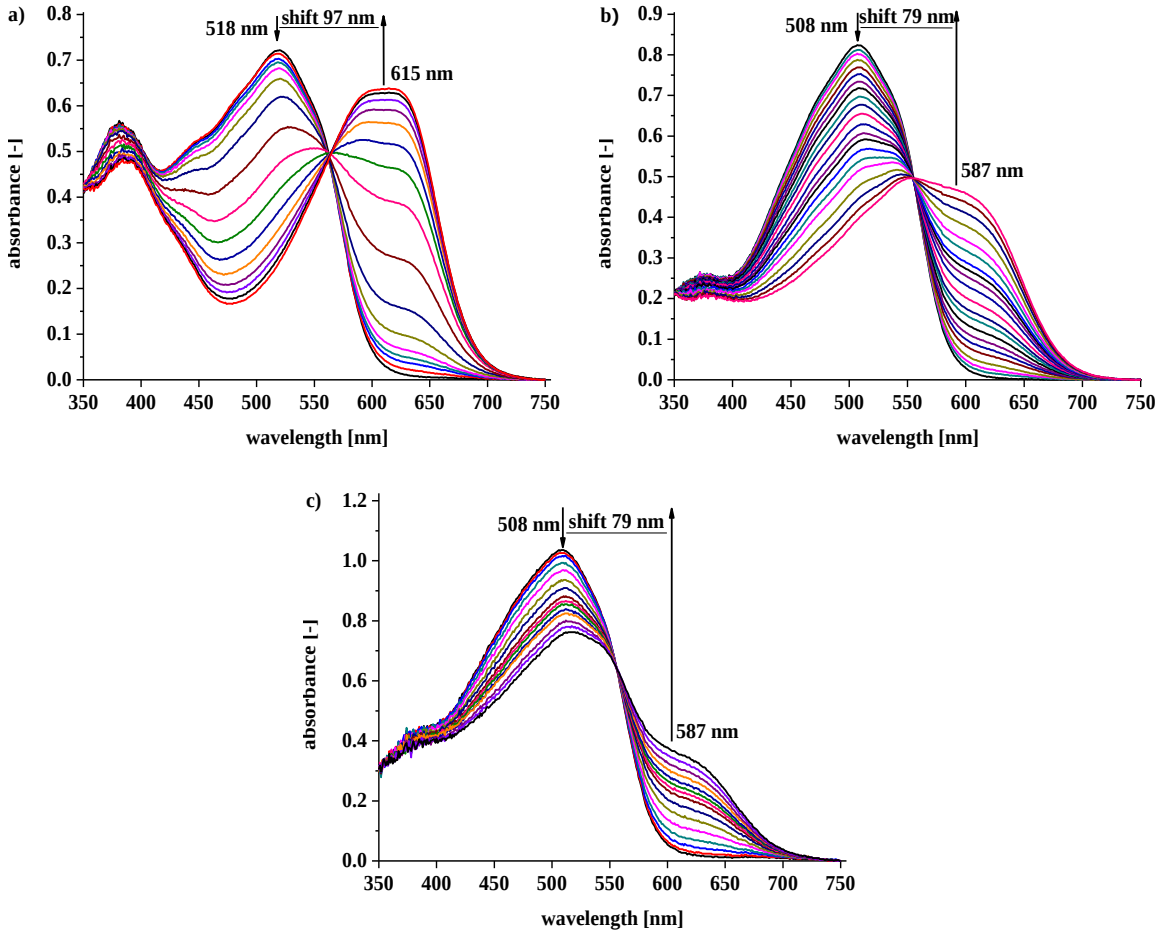

Fig. 3. Changes in UV-Vis spectra of optodes based on diazocrowns: a) **1**, b) **2** and c) **4**, upon titration with aqueous lead(II) nitrate solution in the concentration range of 0 – 1.25×10^{-3} M, 0 – 2.75×10^{-3} M, and 0 – 1.83×10^{-3} M, respectively.

3.2.1. Effect of pH

Aqueous solutions of lead(II) nitrate are undergoing hydrolysis and form hydroxides at pH higher than 5.5 [68-70]. Thus the response of the optodes towards lead(II) obviously can be

expected to be influenced by pH. The response of optodes at lead(II) concentration 10^{-4} M in pH range 1–12 (nitric acid/sodium hydroxide) solutions was studied. The response signal (ΔA) increases with the increase of pH in range from 1 to 10 (Fig. S6). Above pH 10 the decrease of signal was observed, which might be connected with the ionization of chromoionophore and its elution from the polymer matrix. Taking all above into account, all further studies were carried out under pH 5.50±0.05.

3.2.3. Response time, reversibility, repeatability and life time

Response time is one of the important factors when considering the applicability of optodes as sensors. To determine the response time, experiments using membranes immersed in solution of lead(II) (10^{-4} M, pH 5.5) with contact time up to 15 min. were carried out. ΔA of the optodes as a function of time needed for constant optical signal is shown in Fig. S7. The membranes were found to reach 95% of the final signal (t_{95}) within 7 min for optodes with compound **1**, and 3 min for membranes with crowns **2** and **4**. This may be the effect of differences in membrane composition, namely the higher ratio of plasticizer in membranes **2** and **4** comparing membrane **1** affecting the mobility of membrane constituents [63].

The possibility of regeneration of optodes after use - to make them reusable - was checked using as regeneration solutions of HNO_3, HCl, CH_3COOH, EDTA-Na_2 and EDA (10^{-1} and 10^{-2} M). Regeneration time for optodes with compounds **2** and **4**, was 30 seconds, when using HNO_3 or HCl (10^{-1} M). For membrane with crown **1**, the regeneration time was 2 min. In EDTA-Na_2 and EDA solutions the regeneration time was over 30 min and moreover complete regeneration of membranes was not possible (cf. Fig. S8). Thus 10^{-1} M nitric acid was selected for optodes regeneration. After regeneration, optodes were washed three times with deionized water. In Fig. 4 regeneration of optodes is shown for all prepared membranes. After ten cycles a drift of optical signal was less than 1% for optodes with crows **2** and **4**, and less than 4% after five cycles for membranes with compound **1**.

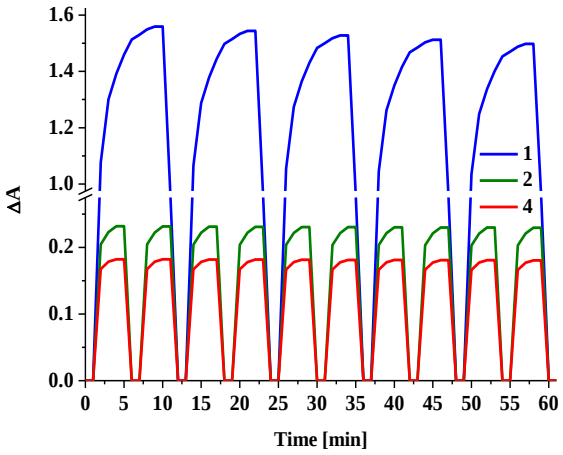

Fig. 4. Regeneration cycles for optodes with crowns **1**, **2** and **4** in 0.1 M HNO_3 solution after contact with lead(II) nitrate solution (10^{-4} M, pH 5.5).

The reproducibility of optodes was evaluated by comparing the ΔA values of the lead(II) loaded membrane samples obtained in the different series for two concentrations 10^{-5} and 10^{-4} M are shown on Fig. 5. The relative standard deviations for the measured ΔA values for 10^{-5} (n = 10) and 10^{-4} M (n = 10), were 1.1% and 1.5% for optodes with crown **1**, 1.0% and 1.6% for optodes with crown **2**, 1.3% and 1.8% for optodes with crown **4**, respectively.

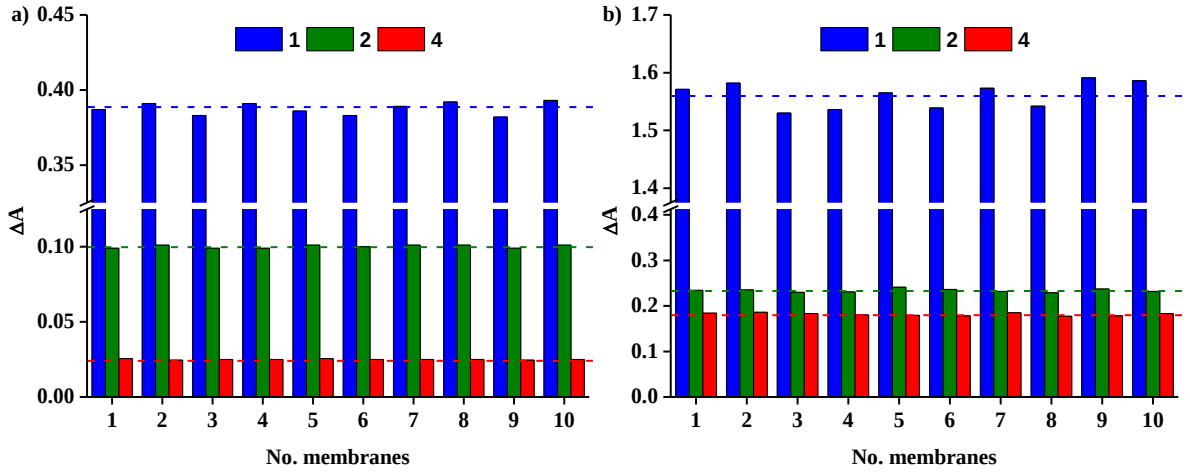

Fig. 5 Reproducibility of optodes with crowns **1**, **2** and **4** after contact with lead(II) nitrate solution a) 10^{-5} M and b) 10^{-4} M (pH 5.5).

The life time of all membranes was determined by immersing membranes in nitric acid solution and measuring the value of ΔA over time, i.e. after: 1, 2, 4, 8, 24, 48, 72, 168 (7 days) and 336 h (14 days). No significant loss of signal was found. Membranes were found to be insensitive to sunlight after 14 days. Membranes that were used and left to dry out typically for cellulose triacetate material undergo deformation, losing their mechanical properties (mainly flexibility). Thus between measurements optodes should be kept in solution,

preferentially in nitric acid solution. Just prepared optodes and not used for measurements can be stored safely for a period of at least 3 months in a dry and dark place (room conditions) without losing their properties (Fig. S9).

3.2.4. Effect of interfering ions

The response of prepared optodes was investigated in the presence of several interfering metal ions: Na^{+}, K^{+}, Ca^{2+}, Mg^{2+}, Ni^{2+}, Cu^{2+}, Zn^{2+}, Cd^{2+}. Fig. 6 shows the influence of addition of 10-fold molar excess of interfering ion salt on the generated signal ΔA of optodes immersed in 10^{-4} M solution of lead(II) nitrate (pH 5.5), as RR% value. Only in the presence of copper(II) RR% value exceeds 5%, however just in case of optode with 21-membered crown **2** as chromoionophore this value is higher than 30%. For **1** and **4** the interference from copper is about 6%. The interference from copper(II) is not surprising, taking into account the agreement with results obtained in metal cation complexation studies in solution for crowns **1**, **2** and **4** [53].

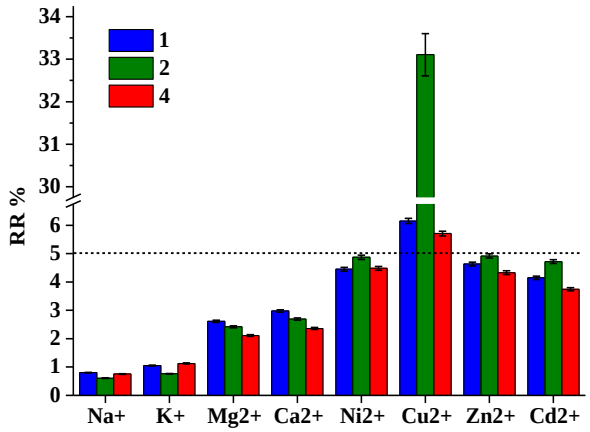

Fig. 6. Interferences of several metal cations (used in 10-fold molar excess), expressed as RR%, to spectral response (ΔA) of optodes with chromoionophores **1** (at 615 nm), **2** (at 587 nm) and **4** (at 587 nm) towards lead(II) nitrate (pH 5.5).

3.2.5. Linear response range

The optical response ΔA of prepared optodes depending on the used chromoionophore show various ranges of linear responses to lead(II) concentration as it is shown in Fig. 7 and Fig.8. For optode with crown **1** (Fig. 7) linear response was found for lead(II) concentration range of 8.05×10^{-8} – 2.24×10^{-5} M with a regression equation of ΔA = 34741.2133[Pb(II)] + 0.0069 (R^2 = 0.998) and detection limit 1.15×10^{-8} M. At concentration ca. 2.0×10^{-3} M sensor riches saturation with analyte. For optodes with chromoionophores **2** and **4** the linear response range of ΔA vs. lead(II) concentration was found to be relatively narrow. Thus the use of

semilogarithmic calibration curves for low concentrations seems to be more convenient (Fig. 8). Then linear response range for optode with compound **1** in semilogarithmic scale covers concentrations 7.86×10^{-6} – 3.83×10^{-4} M, for **2** 1.51×10^{-6} – 2.02×10^{-4} M and for **4** 4.00×10^{-5} – 1.83×10^{-3} M, with regression equations $\Delta A = 1.1639\log[Pb(II)] + 6.1962$ ($R^2 = 0.999$), $\Delta A = 0.1248\log[Pb(II)] + 0.7245$ ($R^2 = 0.996$) and $\Delta A = 0.2071\log[Pb(II)] + 0.9836$ ($R^2 = 0.995$) for **1**, **2** and **4**, respectively. The detection limit of the sensor membranes (n = 10) was found to be 4.79×10^{-6} M, 1.84×10^{-6} M and 2.03×10^{-5} M, for optodes with crowns **1**, **2** and **4**, respectively.

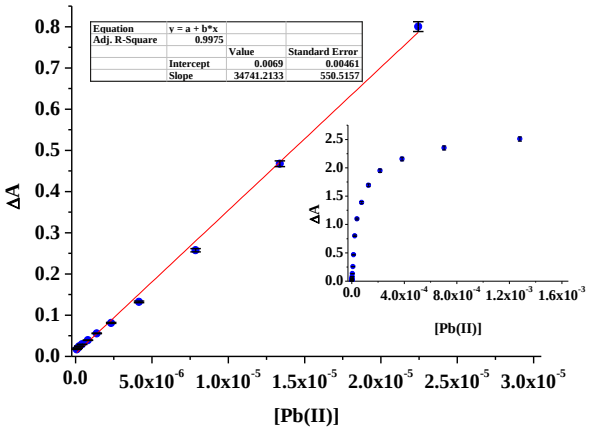

Fig. 7. The optical response ΔA of prepared optodes with chromoionophores **1** to lead(II) concentration. Insets: full range of response.

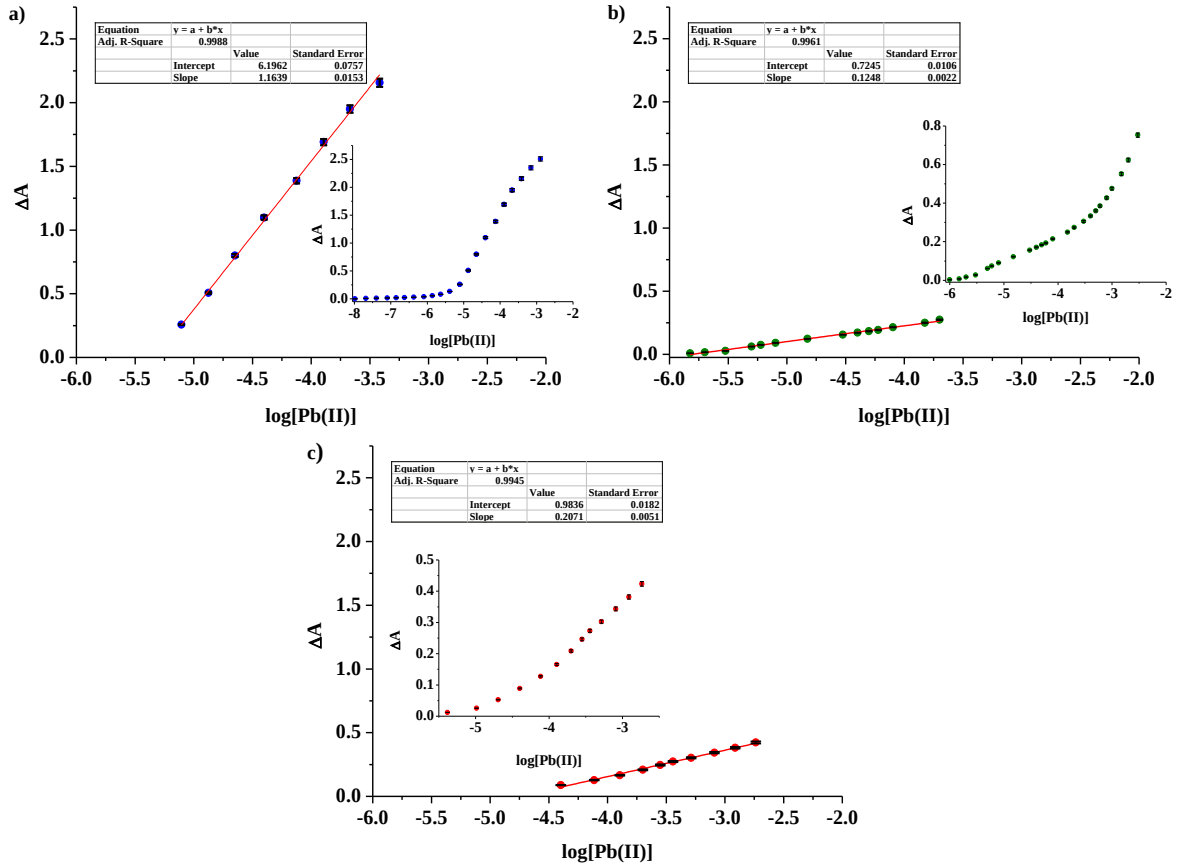

Fig. 8. Calibration curves of optodes with chromoionophores a) **1**, b) **2** and c) **4**. Insets: full range of response.

3.3. Comparison of optodes with already existing ones

In Table 2 the properties of lead(II) selective optodes described in literature [71-81] are listed for comparison with the characteristics of membranes obtained in our studies. From this comparison it is quite well seen that optodes obtained by us are, in general, more or less comparable with those proposed by other authors. However, saying that, the optode with 18-membered macrocycle **1** having comparable LOD value and the range of linear response coming along with relatively short response time can compete with most of the optodes listed in Table 2.

Table 2. Comparison of obtained optodes with already existing ones.

Sensing material	Support	Dynamic range [Pb(II)]	LOD [Pb(II)]	Response time [min]	Reference
ETH 5435 + ETH 5418	PVC	5.0×10^{-9}-5.0×10^{-5}	3.2×10^{-12}	order of minutes	[71]
ETH 5493 + ETH 2439	PVC	1.0×10^{-7}-5.0×10^{-2}	N/D	N/D	[72]
PAN + Dibenzodiaza-18-crown-6	PVC	1.0×10^{-8}-5.0×10^{-5}	1.0×10^{-8}	20	[73]

KTBPE* + Dibenzo-18-crown-6	PVC	1.0×10^{-5}-1.0×10^{-4}	8.0×10^{-6}	15	[74]
ACAD**	CTA	1.0×10^{-6}-5.0×10^{-1}	6.9×10^{-7}	10	[75]
Diphenylcarbazone	PVC	6.9×10^{-6}-1.1×10^{-2}	6.5×10^{-6}	3	[76]
4-hydroxy salophen	CTA	1.0×10^{-7}-1.0×10^{-3}	8.6×10^{-8}	10	[77]
Lead ionophore IV + ETH 5294	PVC	6.2×10^{-8}-5.0×10^{-5}	2.5×10^{-8}	30	[78]
Dithizone	CTA	2.4×10^{-6}-2.7×10^{-5}	7.3×10^{-7}	11-15	[79]
Dithizone	Agarose	1.2×10^{-8}-2.4×10^{-6}	4.0×10^{-9}	28	[80]
Dithizone	Chitosan-Silica	9.7×10^{-7}-5.3×10^{-6}	5.3×10^{-7}	3	[81]
1	CTA	8.1×10^{-8}-2.2×10^{-5}	1.2×10^{-8}	7	This work
2	CTA	1.5×10^{-6}-2.0×10^{-4}	1.8×10^{-6}	3	This work
4	CTA	4.0×10^{-5}-1.8×10^{-3}	2.0×10^{-5}	3	This work

* 3′,3″,5′,5″-Tetrabromophenolphthalein ethyl ester potassium salt

** 2-amino-cyclopentene-1-dithiocarboxylic acid

3.4. Digital image colorimetry

The colorimetric analysis of the digital images was carried out in parallel with the study of the spectrophotometric response of the optodes. Fig. 9 show color changes of optodes with chromoionophores **1**, **2** and **4** after contact with solutions of different concentrations of lead(II) nitrate at pH 5.5. Photos were taken using a Smartphone camera. The most visible color changes, which can be traced by "the naked eye" were observed in the case of the membrane with compound **1**. In the case of materials with chromoionophores **2** and **4** the observed color changes were not spectacular, especially for membranes with crown **4**. Fig. 9a shows the dependence of color change (ΔE_{RGB}) vs. log[Pb(II)] for optode with compound **1** with the dynamic range covering concentration range 7.79×10^{-7} – 2.07×10^{-4} M and regression equation ΔE_{RGB} = 58.44log[Pb(II)] + 357.44 (R^2 = 0.997). For membranes with crown **2** (Fig. 9b) the calibration curve in a semilogarithmic scale is linear within 2.37×10^{-5} to 7.10×10^{-4} M of lead(II) salt and calibration curve can be expressed with equation of ΔE_{RGB} = 25.39log[Pb(II)] + 122.01 (R^2 = 0.995). The response of the optode with compound **4** (Fig. 9c) towards lead(II) can be described by equation ΔE_{RGB} = 15.72×[Pb(II)] + 75.85 (R^2 = 0.997) with linear range of response in the concentration range of 2.04×10^{-5} – 1.83×10^{-3} M of Pb(II). For detailed data see Tables S4-S6. Comparing slopes of obtained calibration curves, optode **1** characterizes with the highest sensitivity among investigated materials. The

detection limits (LOD) are 8.62×10^{-7} M, 2.05×10^{-5} M and 2.33×10^{-5} M for membranes with diazocrowns **1**, **2** and **4**, respectively.

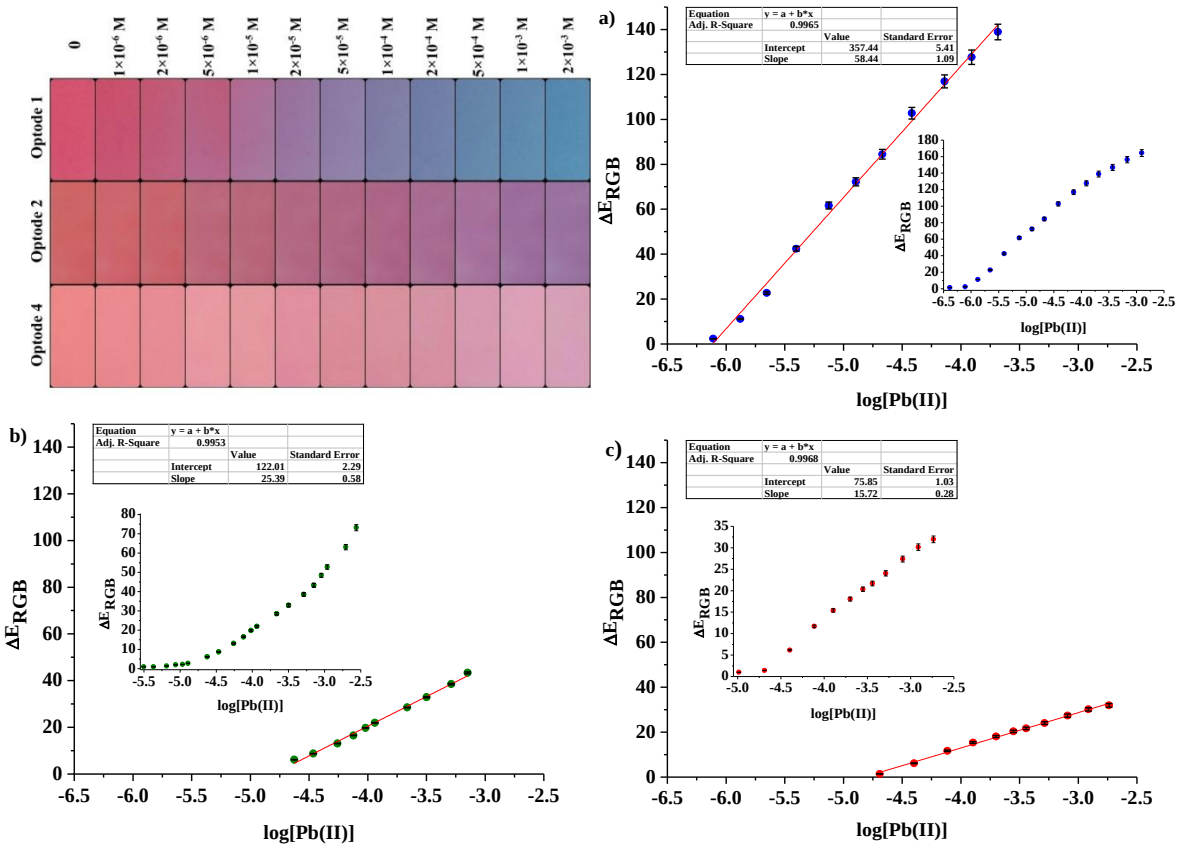

Fig. 9. Left upper corner: Color change of membranes with chromoionophores **1**, **2** and **4** after contact with aqueous lead(II) nitrate at different concentrations (pH 5.5). Calibration curves for membranes with chromoionophores a) **1**, b) **2** and c) **4** as a function of the color change (ΔE_{RGB}) vs. log[Pb(II)] (pH 5.5) Insets: full range response.

3.5. Analytical performance - determination of Pb(II) in model and real samples

Applications of proposed optodes were tested using different samples: of known lead(II) concentrations – commercial lead(II) standard solution, spiked tap water from different regions of northern Poland, and real industrial sample of treated wastewater of unknown elemental composition. In the last case results were compared with the values obtained by independent analysis using ICP-OES. As a sensor, optode with chromoionophore **1** was chosen, as material of the best properties among all obtained optodes. All measurements were done at pH 5.5. Both attempts were tested: spectrophotometric (ΔA) and colorimetric (ΔE_{RGB}) detection of lead(II) using a calibration curve method.

Comparison of recovery results obtained for optodes with chromoionophore **1** upon immersion of the sensor layer in a commercial standard lead(II) solution (SRM) of different

concentrations are collected in Table 3. The recoveries are at least about 98.97 – 101.59% (n = 5) for spectrophotometric detection (ΔA) for lead(II) concentrations in range from 4.83×10^{-8} M (10 ppb) to 4.83×10^{-6} M (1000 ppb). Colorimetric determination is possible at concentration 4.83×10^{-6} M (1000 ppb) with recovery 100.96% (n = 5). To evaluate the influence of the sample matrix three different samples of tap water were spiked with known concentration of lead(II) - Table 3. In this case recoveries were within 98.96 – 101.65% (n = 5) for spectrophotometric detection (ΔA) and 101.24 – 102.28% (n = 5) for Digital Color Analysis attempt (ΔE_{RGB}).

Table 3. Determination of lead(II) ions by optode with compound **1** - recovery test for commercial Standard Reference Solution, and in a real sample - spiked tap water.

	Added Pb(II)		Found Pb(II)							
			ΔA		Recovery	RSD	ΔE_{RGB}		Recovery	RSD
	[Pb(II)]	ppb	[Pb(II)]	ppb	%	%	[Pb(II)]	ppb	%	%
Standard Reference Solution of lead(II)	4.76×10^{-8}	9.864	4.84×10^{-8}	10.010	101.59	2.70	<LOD		-	-
	9.94×10^{-8}	20.580	9.90×10^{-8}	20.497	99.60	1.59	<LOD		-	-
	2.43×10^{-7}	50.376	2.45×10^{-7}	50.646	100.82	0.94	<LOD		-	-
	4.86×10^{-7}	100.650	4.81×10^{-7}	99.564	98.97	0.61	<LOD		-	-
Tap water 1	-	-	<LOD		-	-	<LOD		-	-
	4.83×10^{-8}	10.00	4.78×10^{-8}	9.89	98.93	3.26	<LOD		-	-
	4.83×10^{-7}	100.00	4.80×10^{-7}	99.39	99.40	0.34	<LOD		-	-
	4.83×10^{-6}	1000.00	4.85×10^{-6}	1004.58	100.48	0.30	4.89×10^{-6}	1012.32	101.25	0.41
Tap water 2	-	-	<LOD		-	-	<LOD		-	-
	4.83×10^{-8}	10.00	4.89×10^{-8}	10.13	101.31	2.11	<LOD		-	-
	4.83×10^{-7}	100.00	4.84×10^{-7}	100.22	100.22	0.65	<LOD		-	-
	4.83×10^{-6}	1000.00	4.90×10^{-6}	1014.71	101.49	0.45	4.92×10^{-6}	1018.88	101.91	0.57
Tap water 3	-	-	<LOD		-	-	<LOD		-	-
	4.83×10^{-8}	10.00	4.86×10^{-8}	10.07	101.31	2.49	<LOD		-	-
	4.83×10^{-7}	100.00	4.78×10^{-7}	99.03	99.05	0.50	<LOD		-	-
	4.83×10^{-6}	1000.00	4.91×10^{-6}	1016.49	101.67	0.36	4.90×10^{-6}	1014.71	101.49	0.27

The last probe for testing practical application of the proposed sensor layer was using optode with chromoionophore **1** for spectrophotometric detection of lead(II) in real wastewater sample of the elemental composition shown in Table S7. Trace elements were determined by the ICP-OES method.

In Table 4 results of the recovery test are collected. Recovery when the calibration curve method was used is 96.25% (n = 5), whereas standard addition method was applied the recovery was 99.06 – 100.62% (n = 5).

Table 4. Determination of lead(II) in treated industrial wastewater using optode with compound **1**.

	ICP-OES		Added Pb(II)		Found Pb(II) ΔA		Recovery	RSD
	[Pb(II)]	ppb	[Pb(II)]	ppb	[Pb(II)]	ppb	%	%
Industrial wastewater	9.51×10^{-8}	19.70	-	-	9.15×10^{-8}	18.95	96.25[a]	3.95
			9.66×10^{-8}	20.00	1.90×10^{-7}	39.33	99.06[b]	1.19
			2.42×10^{-7}	50.00	3.39×10^{-7}	70.13	100.62[b]	0.57

a - calibration curve, b - standard addition method

Analysis of the recovery test shows successful agreement between our results and the results obtained by both comparison with SRM and obtained by ICP-OES method. It can be concluded that sensing membrane with chromoionophore **1** can be a useful - fast and reliable - analytical tool for detection and determination of lead(II) in aqueous samples.

4. Conclusion

Pyrrole bearing diazocrowns **1-4** of different macrocycle size and type of linkers were tested as chromoionophores in optodes based on cellulose triacetate matrix. The best properties: linear response range and detection limit presents sensor material where 18-membered derivative bearing oligoether moiety was used. The obtained optode can be used for the detection and determination of lead(II) in environmental samples, both as a quick qualitative test and for quantitative determination of analyte. Both laboratory applications and also field analyses are worth considering by use of mobile spectrophotometers and using free of charge color application for mobile devices. It might be said that proposed by us, an easy and cheap solution can be considered as at least complementary, if not competitive, for routinely used in environmental analysis methods such as AAS or ICP-OES, which are not only expensive with equipment, but also require well trained staff. To sum up, the proposed optodes can be used for routine analysis of water samples also with portable equipment.

CRediT author statement

Błażej Galiński: planning and carrying out of all measurements; data working-up; calculations and visualization; draft interpretation of results, writing draft manuscript; **Ewa Wagner-Wysiecka**: the main conceptual ideas, interpretation and verification of results, writing&editing of the final version, writing - review, supervising project. **Both authors** discussed the results and contributed to the final manuscript.

Declaration of Competing Interest

The authors declare that they have no known competing financial interests or personal relationships that could have appeared to influence the work reported in this paper.

Acknowledgments

This work was supported by the Faculty of Chemistry, Gdańsk University of Technology, No. 034718 and 035138 - an internal grants from statutory funds. The authors are grateful to anonymous reviewers for their careful review, which helped us to improve the quality of the above manuscript.

References

[1] R.S. Boyd RS, Heavy metal pollutants and chemical ecology: exploring new frontiers, J. Chem. Ecol. 36 (2010) 46-58. https://doi.org/10.1007/s10886-009-9730-5.

[2] K. Jomova, M. Valko M, Advances in metal-induced oxidative stress and human disease, Toxicology 283 (2011) 65-87. https://doi.org/10.1016/j.tox.2011.03.001.

[3] P.B. Tchounwou, C.G. Yedjou, A.K. Patlolla, D.J. Sutton, Heavy metal toxicity and the environment, in: A. Luch (Eds.), Molecular, Clinical and Environmental Toxicology, Springer, Basel, 2012 pp. 133-164. https://doi.org/10.1007/978-3-7643-8340-4_6.

[4] S. Squadrone, M. Prearo, P. Brizio, S. Gavinelli, M. Pellegrino, T. Scanzio, S. Guarise, A. Benedetto, M.C. Abete, Heavy metals distribution in muscle, liver, kidney and gill of European catfish (*Silurus glanis*) from Italian rivers, Chemosphere 90 (2013) 358-365. https://doi.org/10.1016/j.chemosphere.2012.07.028.

[5] B.E. Belabed, A. Meddour, B. Samraoui, H. Chenchouni, Modeling seasonal and spatial contamination of surface waters and upper sediments with trace metal elements across industrialized urban areas of the Seybouse watershed in North Africa, Environ. Monit. Assess. 189 (2017) 265. https://doi.org/10.1007/s10661-017-5968-5.

[6] Y. Gan, X. Huang, S. Li, N. Liu, Y.C. Li, A. Freidenreich, W. Wang, R. Wang, J. Dai, Source quantification and potential risk of mercury, cadmium, arsenic, lead, and chromium in farmland soils of Yellow River Delta, J. Clean. Prod. 221 (2019) 98-107. https://doi.org/10.1016/j.jclepro.2019.02.157.

[7] P. Neelam, P. Sumit, M. Anushree, D.K. Singh, Impact assessment of contaminated River Yamuna water irrigation on soil and crop grown in peri-urban area of Delhi-NCR, Environ. Conserv. J. 20 (2019) 99-112. https://doi.org/10.36953/ECJ.2019.20314.

[8] S.C. Obiora, A. Chukwu, T.C. Davies, Contamination of the potable water supply in the lead–Zinc mining communities of Enyigba, Southeastern Nigeria, Mine. Water. Environ. 38 (2019) 148-157. https://doi.org/10.1007/s10230-018-0550-0.

[9] H. Peng, Y. Chen, L. Weng, J. Ma, Y. Ma, Y. Li, M.S. Islam, Comparisons of heavy metal input inventory in agricultural soils in north and south China: a review, Sci. Total. Environ. 660 (2019) 776-786. https://doi.org/10.1016/j.scitotenv.2019.01.066.

[10] H. Can, I.I. Ozyigit, M. Can, A. Hocaoglu-Ozyigit, I.E. Yalcin, Environment-based impairment in mineral nutrient status and heavy metal contents of commonly consumed leafy vegetables marketed in Kyrgyzstan: a case study for health risk assessment, Biol. Trace. Elem. Res. 199 (2020) 1123-1144. https://doi.org/10.1007/s12011-020-02208-6.

[11] C. Ma, F. Liu, P. Xie, K. Zhang, J. Yang, J. Zhao, H. Zhang, Mechanism of Pb absorption in wheat grains, J. Hazard. Mater. 415 (2021) 125618. https://doi.org/10.1016/j.jhazmat.2021.125618.

[12] G. Le Roux, F. De Vleeschouwer, D. Weiss, O. Masson, E. Pinelli, W. Shotyk, Learning from the Past: Fires, Architecture, and Environmental Lead Emissions, Environ. Sci. Technol. 53 (2019) 8482-8484. https://doi.org/10.1021/acs.est.9b03869.

[13] K.E. Smith, D. Weis, C. Chauvel, S. Moulin, Honey Maps the Pb Fallout from the 2019 Fire at Notre-Dame Cathedral, Paris: A Geochemical Perspective, Environ. Sci. Technol. Lett. 7 (2020) 753–759. https://doi.org/10.1021/acs.estlett.0c00485.

[14] A. van Geen, Y. Yao, T. Ellis, A. Gelman, Fallout of Lead Over Paris From the 2019 Notre-Dame Cathedral Fire, GeoHealth 4 (2020) e2020GH000279. https://doi.org/10.1029/2020GH000279.

[15] N. Date, A. Sato, K. Takeuchi, T. Mori, K. Yokosuka, Y. Ito, K. Shima, K. Suzuki, H. Taguchi, T. Chiyozaki, K. Yanagawa, T.K. Giles, T. Akitsu, Fire at Notre Dame Cathedral and Lead Materials in the Environment, Fire Sci. Technol. 39 (2020) 17-37. https://doi.org/10.3210/fst.39.17.

[16] P. Glorennec, A. Azema, S. Durand, S. Ayrault, B. Le Bot, The Isotopic Signature of Lead Emanations during the Fire at Notre Dame Cathedral in Paris, France, Int. J. Environ. Res. Public Health 18 (2021) 5420. https://doi.org/10.3390/ijerph18105420.

[17] A. Vallée, E. Sorbets, H. Lelong, J. Langrand, J. Blacher, The lead story of the fire at the Notre-Dame cathedral of Paris, Environ. Pollut. 269 (2021), 116140. https://doi.org/.1016/j.envpol.2020.116140.

[18] A. Allonneau, S. Mercier, O. Maurin, F. Robardet, A. Menguy-Fleuriot, S.-C. Luu, C. Louyot, N. Jacques, R. Jouffroy, B. Prunet, Lead contamination among Paris Fire Brigade firefighters who fought the Notre Dame Cathedral fire in Paris, Int. J. Hyg. Environ. Health. 233 (2021) 113707. https://doi.org/10.1016/j.ijheh.2021.113707.

[19] I. Yaroshenko, D. Kirsanov, M. Marjanovic, P.A. Lieberzeit, O. Korostynska, A. Mason, I. Frau, A. Legin, Real-Time water quality monitoring with chemical sensors, Sensors 20 (2020) 3432. https://doi.org/10.3390/s20123432.

[20] J. Tan, J. Xie, Applications of electronic nose (e-nose) and electronic tongue (e-tongue) in food quality-related properties determination: A review. Arti. Intell. Agric. 4 (2020) 104-115. https://doi.org/10.1016/j.aiia.2020.06.003.

[21] J. Saini, M. Dutta, G. Marques, Sensors for indoor air quality monitoring and assessment through Internet of Things: a systematic review, Environ. Monit. Assess. 193 (2021) 66. https://doi.org/10.1007/s10661-020-08781-6.

[22] J. Perumal, Y. Wang, A. Binte Ebrahim Attia, U. S. Dinish, M. Olivo, Towards a point-of-care SERS sensor for biomedical and agri-food analysis applications: a review of recent advancements, Nanoscale 13 (2021) 553-580. https://doi.org/10.1039/D0NR06832B.

[23] C. McDonagh, C.S. Burke, B.D. MacCraith, Optical chemical sensors, Chem. Rev. 108 (2008) 400-422. https://doi.org/10.1021/cr068102g.

[24] A. Lobnik, M. Turel, S.K. Urek, Optical chemical sensors: design and applications, in: W. Wang (Eds.), Advances in chemical sensors, InTech, 2012 pp. 3-28. https://doi.org/10.5772/31534.

[25] G. Mistlberger, G.A. Crespo, E. Bakker, Ionophore-based optical sensors, Annu. Rev. Anal. Chem. 7 (2014) 483-512. https://doi.org/10.1146/annurev-anchem-071213-020307.

[26] X Xie, E. Bakker, Ion selective optodes: from the bulk to the nanoscale, Anal. Bioanal. Chem. 407 (2015) 3899-3910. https://doi.org/10.1007/s00216-014-8413-4.

[27] K.N. Mikhelson, M.A. Peshkova, Advances and trends in ionophore-based chemical sensors, Russ. Chem. Rev. 84 (2015) 555-578. https://doi.org/10.1070/RCR4506.

[28] I.I. Ebralidze, N.O. Laschuk, J. Poisson, O.V. Zenkina, Colorimetric sensors and sensor arrays, in: O.V. Zenkina (Eds.), Nanomaterials design for sensing applications, Elsevier, 2019 pp. 1-39. https://doi.org/10.1016/B978-0-12-814505-0.00001-1.

[29] X. Du, X. Xie, Ion-Selective optodes: Alternative approaches for simplified fabrication and signaling, Sens. Actuators B Chem. 335 (2021) 129368. https://doi.org/10.1016/j.snb.2020.129368.

[30] X. Du, X. Xie, Non-equilibrium diffusion controlled ion-selective optical sensor for blood potassium determination, ACS Sens. 2 (2017) 1410-1414. https://doi.org/10.1021/acssensors.7b00614.

[31] A. Kalinichev , M. Peshkova, N. Pokhvishcheva, K. Mikhelson, Ion-selective optical sensors: a new look at well-established techniques of signal acquisition, Proceedings, 2 (2018) 825. https://doi:10.3390/proceedings2130825.

[32] G. Albizu, A. Bordagaray, S. Dávila, R. Garcia-Arrona, M. Ostra, M. Vidal, Analytical control of nickel coating baths by digital image analysis, Microchem. J. 154 (2020) 104600. https://doi.org/10.1016/j.microc.2020.104600.

[33] N. Yu. Tiuftiakov, A. V. Kalinichev, N. V. Pokhvishcheva, M.A. Peshakova, Digital color analysis for colorimetric signal processing: Towards an analytically justified choice of

acquisition technique and color space, Sensors and Actuators B, 344 (2021) 130274. https://doi.org/10.1016/j.snb.2021.130274.

[34] S. Upadhyay, A. Singh, R. Sinha, S. Omer, K. Negi, Colorimetric chemosensors for d-metal ions: A review in the past, present and future prospect, J. Mol. Struct. 1193 (2019) 89-102. https://doi.org/10.1016/j.molstruc.2019.05.007.

[35] G. Fukuhara, Analytical supramolecular chemistry: Colorimetric and fluorimetric chemosensors, J. Photochem. Photobiol. C 42 (2020) 100340. https://doi.org/10.1016/j.jphotochemrev.2020.100340.

[36] U.E. Spichiger, D. Freiner, E. Bakker, T. Rosatzin, W. Simon, Optodes in clinical chemistry: potential and limitations, Sens. Actuators B Chem. 11 (1993) 263-271. https://doi.org/10.1016/0925-4005(93)85264-B.

[37] H.N. Kim, W.X. Ren, J.S. Kim, J. Yoon, Fluorescent and colorimetric sensors for detection of lead, cadmium, and mercury ions, Chem. Soc. Rev. 41 (2012) 3210-3244. https://doi.org/10.1039/C1CS15245A.

[38] K.L. Diehl, E.V. Anslyn, Array sensing using optical methods for detection of chemical and biological hazards, Chem. Soc. Rev. 42 (2013) 8596-8611. https://doi.org/10.1039/C3CS60136F.

[39] L. You, D. Zha, E.V. Anslyn, Recent advances in supramolecular analytical chemistry using optical sensing, Chem. Rev. 115 (2015) 7840-7892. https://doi.org/10.1021/cr5005524.

[40] H. Sharma, N. Kaur, A. Singh, A. Kuwar, N. Singh, Optical chemosensors for water sample analysis, J. Mater. Chem. C 4 (2016) 5154-5194. https://doi.org/10.1039/C6TC00605A.

[41] P.V.S. Ajay, J. Printo, D.S.C.G. Kiruba, L. Susithra, K. Takatoshi, M. Sivakumar, Colorimetric sensors for rapid detection of various analytes, Mater. Sci. Eng. C 78 (2017) 1231-1245. https://doi.org/10.1016/j.msec.2017.05.018.

[42] M.J. Kangas, R.M. Burks, J. Atwater, R.M. Lukowicz, P. Williams, A.E. Holmes, Colorimetric sensor arrays for the detection and identification of chemical weapons and explosives, Crit. Rev. Anal. Chem. 47 (2017) 138-153.
https://dx.doi.org/10.1080/10408347.2016.1233805.

[43] Y. Ma, Y. Li, K. Ma, Z. Wang, Optical colorimetric sensor arrays for chemical and biological analysis, Sci. China Chem. 61 (2018) 643-655. https://doi.org/10.1007/s11426-017-9224-3.

[44] K. Koren, S. E. Zieger, Optode based chemical imaging-possibilities, challenges, and new avenues in multidimensional optical sensing, ACS Sens. 6 (2021) 1671–1680. https://doi.org/10.1021/acssensors.1c00480.

[45] S. Kumar, R. Singh, Recent optical sensing technologies for the detection of various biomolecules: Review. Opt. Laser. Technol. 134 (2021) 106620. https://doi.org/10.1016/j.optlastec.2020.106620.

[46] T. Minami, Design of Supramolecular Sensors and Their Applications to Optical Chips and Organic Devices. Bull. Chem. Soc. Jpn. 94 (2021) 24-33. https://doi.org/10.1246/bcsj.20200233.

[47] E. Wagner-Wysiecka, N. Łukasik, J.F. Biernat, E. Luboch, Azo group(s) in selected macrocyclic compounds, J. Incl. Phenom. Macrocyl. Chem. 90 (2018) 189-257. https://doi.org/10.1007/s10847-017-0779-4.

[48] E. Wagner-Wysiecka, E. Luboch, M. Kowalczyk, J.F. Biernat, Chromogenic macrocyclic derivatives of azoles - synthesis and properties, Tetrahedron 59 (2003) 4415-4420. https://doi.org/10.1016/S0040-4020(03)00618-5.

[49] E. Wagner-Wysiecka, E. Luboch, M. Jamrógiewicz, J. Szczygelska-Tao, J.F. Biernat, Metallochromic azole azomacrocyclic reagents, Ann. Pol. Chem. Soc. 4 (2005) 11-14.

[50] E. Luboch, E. Wagner-Wysiecka, M. Fainerman-Melnikova, L.F. Lindoy, J.F. Biernat, Pyrrole azocrown ethers. Synthesis, complexation, selective lead transport and ion-selective membrane electrode studies, Supramol. Chem. 18 (2006) 593-601. https://doi.org/10.1080/10610270600879068.

[51] E. Wagner-Wysiecka, E. Luboch, M. Fonari, The synthesis, X-ray structure and metal cation complexation properties of colored crown with two heterocyclic residues as a part of macrocycle. Pol. J. Chem. 82, (2008) 1319-1330.

[52] E. Luboch, E. Wagner-Wysiecka, T. Rzymowski, M. Fonari, R. Kulmaczewski, Pyrrole azocrown ethers - synthesis, crystal structures, and fluorescence properties. Tetrahedron, 67 (2011) 1862-1872. https://doi.org/10.1016/j.tet.2011.01.027.

[53] B. Galiński, E. Luboch, J. Chojnacki, E. Wagner-Wysiecka, Novel diazocrowns with pyrrole residue as lead(II) colorimetric probes. Materials, 14, (2021) 7239. https://doi.org/10.3390/ma14237239.

[54]

https://play.google.com/store/apps/details?id=com.leizersoft.coloranalysis&hl=pl&gl=US

[55] N.A. Gavrilenko, S.V. Muravyov, S.V. Silushkin, A.S. Spiridonovab, Polymethacrylate optodes: A potential for chemical digital color analysis, Measurement 51 (2014) 464-469. https://doi.org/10.1016/j.measurement.2013.11.027.

[56] S.V. Muravyov, A.S. Spiridonova, N.A. Gavrilenko, P.V. Baranov, L.I. Khudonogovo, A digital colorimetric analyzer for chemical measurements on the basis of polymeric optodes, Instrum. Exp. Tech. 59 (2016) 592–600. https://doi.org/10.1134/S0020441216030210.

[57] S.V. Muravyov, N.A. Gavrilenko, N.V.Saranchina, P.V. Baranov, Polymethacrylate sensors for rapid digital colorimetric analysis of toxicants in natural and anthropogenic objects, IEEE Sens. J. 19 (2019) 4765-4772. https://doi.org/10.1109/JSEN.2019.2903314.

[58] M.A.D. Rabbani, B. Khalili, H. Saeidian, Novel edaravone-based azo dyes: efficient synthesis, characterization, antibacterial activity, DFT calculations and comprehensive investigation of the solvent effect on the absorption spectra, RSC Adv. 10 (2020) 35729. https://doi.org/10.1039/d0ra06934e.

[59] Y. Peng, Y. Sui, Compatibility research on PVC/PVB blended membranes, Desalination 196 (2006) 13-21. https://doi:10.1016/j.desal.2005.07.053.

[60] G.E. Chen, W.G. Sun, Q. Wu, Y.F. Kong, Z.L. Xu, S. J. Xu, X. P. Zheng, Effect of cellulose triacetate membrane thickness on forward-osmosis performance and application for spent electroless nickel plating baths. J. Appl. Polym. Sci. 38 (2017) 148-157. https://doi.org/10.1007/s10230-018-0550-0.

[61] E. Bakker, M. Willer, M. Lerchi, K. Seller, E. Pretsch, Determination of complex formation constants of neutral cation-selective ionophores in solvent polymeric membranes, Anal. Chem. 66 (1994) 516-521. https://doi.org/10.1021/ac00076a016.

[62] P.C. Meier, W.E. Morf, M. Läubli, W. Simon, Evaluation of the optimum composition of neutral-carrier membrane electrodes with incorporated cation-exchanger sites, Anal. Chim. Acta 156 (1984) 1-8. https://doi.org/10.1016/S0003-2670(00)85531-2.

[63] E. Bakker, P. Bühlmann, E. Pretsch, Carrier-based ion-selective electrodes and bulk optodes. 1. General characteristics, Chem. Rev. 97 (1997) 3083-3132. https://doi.org/10.1021/cr940394a.

[64] O.M. Petrukhin, A. B. Kharitonov, E.V. Frakiisky, Y.I. Urusov, A.F. Zhukov, A.N. Shipway, V.E. Baulin, Effect of lipophilic anionic additives on detection limits of ion-selective electrodes based on ionophores with phosphoryl complexing groups, Sens. Actuators B Chem. 76 (2001) 653-659. https://doi.org/10.1016/S0925-4005(01)00662-1.

[65] D. I. Dekina, A.V. Kalinichev, N.V. Pokhvishcheva, M.A. Peshkova, K.N. Mikhelson, Effects of quantitative composition of the sensing phase in the response of ionophore-based

optical sensors, Sens. Actuators B Chem. 277 (2018) 535-543. https://doi.org/10.1016/j.snb.2018.09.018.

[66] S. L. R. Barker, M. R. Shortreed, R. Kopelman, Utilization of Lipophilic Ionic Additives in Liquid Polymer Film Optodes for Selective Anion Activity Measurements, Anal. Chem. 69 (1997) 990-995. https://doi.org/10.1021/ac960700f.

[67] L. Li, P. Du, Y. Zhang, Y. Qian, P. Zhan, Q. Guo, Intramolecularly hydrogen-bonded cavity containing macrocyclic/acyclic aromatic pyridone foldarands as modularly tunable ionophores for selective potentiometric sensing of metal ions, Sens. Actuators B Chem. 331 (2021) 129385. https://doi.org/10.1016/j.snb.2020.129385.

[68] C.F. Baes, R.S. Mesmer, The hydrolysis of cations, John Wiley & Sons, New York, 1976.

[69] R.N. Sylva, P.L. Brown, The hydrolysis of metal ions. Part 3. Lead(II), J. Chem. Soc., Dalton Trans. 9 (1980) 1577-1581. https://doi.org/10.1039/DT9800001577.

[70] J.J. Cruywagen, R.F. van de Water, The hydrolysis of lead(II). A potentiometric and enthalpimetric study, Talanta 40 (1993) 1091-1095. https://doi.org/10.1016/0039-9140(93)80171-M.

[71] M. Lerchi, E. Bakker, B. Rusterholz, W. Simon, Lead-selective bulk optode based on neutral ionophores with subnanomolar detection limits, Anal. Chem. 64 (1992) 1534-1540. https://doi.org/10.1021/ac00038a007.

[72] E. Anticó, M. Lerchi, B. Rusterholz, N. Achermann, M. Badertscher, M. Valiente, E. Pretsch**,** Monitoring Pb^{2+} with optical sensing films, Anal. Chim. Acta 388 (1999) 327-338. https://doi.org/10.1016/S0003-2670(99)00085-9.

[73] N. Alizadeh, A. Moemeni, M. Shamsipur, Poly(vinyl chloride)-membrane ion-selective bulk optode based on 1,10-dibenzyl-1,10-diaza-18-crown-6 and 1-(2-pyridylazo)-2-naphthol for Cu^{2+} and Pb^{2+} ions, Anal. Chim. Acta 464 (2002) 187-196. https://doi.org/10.1016/S0003-2670(02)00477-4.

[74] Y. Takahashi, T. Hayashita, T.M. Suzuki, Test Strips for Lead(II) Based on a Unique Color Change of PVC-film Containing O-Donor Macrocycles and an Anionic Dye, Anal. Sci. 23 (2007) 147-150. https://doi.org/10.2116/analsci.23.147.

[75] A.A. Ensafi, Z.N. Isfahani, Determination of lead ions by an optical sensor based on 2-amino-cyclopentene-1-dithiocarboxylic acid, IEEE Sens. J. 7 (2007) 1112-1117. https://doi.org/10.1109/JSEN.2007.897942.

[76] A.A. Ensafi, M.Fouladgar, Development a simple PVC membrane bulk optode for determination of lead ions in water samples, Sens. Lett. 7 (2009) 177-184. https://doi.org/10.1166/sl.2009.1029.

[77] A.A. Asnafi, A. Katiraei Far, S. Meghdadi, Highly selective optical-sensing film for lead(II) determination in water samples, J. Hazard. Mater. 172 (2009) 1069-1075. https://doi.org/10.1016/j.jhazmat.2009.07.112.

[78] C. Bualoma, W. Ngeontaeb, S. Nitiyanontakita, P. Ngamukota, A. Imyima, T. Tuntulania, W. Aeungmaitrepirom, Bulk optode sensors for batch and flow-through determinations of lead ion in water samples, Talanta 82 (2010) 660-667. https://doi.org/10.1016/j.talanta.2010.05.028.

[79] H. Tavallali, L. Dorostghoal, Design and evaluation of a lead (II) optical sensor based on immobilization of dithizone on triacetylcellulose membrane, Int. J. Chemtech Res. 6 (2014) 3179-3186.

[80] K. Zargoosh, F.F. Babadi, Highly selective and sensitive optical sensor for determination of Pb(II) and Hg^{2+} ions based on the covalent immobilization of dithizone on agarose membrane, Spectrochim. Acta A Mol. Biomol. Spectrosc. 137 (2015) 105-110. https://doi.org/10.1016/j.saa.2014.08.043.

[81] Y. Nur, E. Rohaeti, L.K. Darusman, Optical sensor for the determination of Pb(II) based on immobilization of dithizone onto chitosan-silica membrane, Indones. J. Chem. 17 (2017) 7-14. https://doi.org/10.22146/ijc.23560.